Chapter 5
The Ginzburg-Landau Equation

Ginzburg-Landau equations have been used to model a wide variety of physical systems (see, e.g., [1]). In the context of pattern formation the *real Ginzburg-Landau equation (RGLE)* was first derived as long-wave *amplitude equation* in the connection with convection in binary mixtures near the onset of instability [44], [50]. The *complex Ginzburg-Landau equation (CGLE)* was first derived in the studies of Poiseuille flow [53] and reaction-diffusion systems [26].
Let us consider the conditions under which the real and complex Ginzburg-Landau equations arise. For simplicity we restrict attention to one spatial dimension. However, the results can be easily generalised to two- and three-dimensional cases.

5.1 The Real Ginzburg-Landau Equation

Let us consider a system

$$\partial_t u = \mathscr{N}(\sigma)u, \qquad u = u(x,t) \tag{5.1}$$

with a nonlinear operator $\mathscr{N}$, depending on some control parameter σ. Suppose that the system (5.1) admits a homogeneous solution $u = u_0$ and (5.1) undergoes a finite-wavelength instability as σ is varied, e.g., becomes positive. That is, if we consider evolution of the Fourier mode $\exp(ikx+\lambda t)$ the growthrate $\mathrm{Re}(\lambda)$ behaves as follows: for $\sigma < 0$ all modes are decaying ($\mathrm{Re}(\lambda) < 0$) and the homogeneous solution u_0 is stable. For $\sigma = 0$, a critical wavenumber k_c gains neutral stability and for $\sigma > 0$ there is a narrow band of wavenumbers around k_c where the growthrate $\mathrm{Re}(\lambda)$ is positive. Let us also assume that the instability we are interested in is *supercritical*, i.e., the nonlinearities saturate so that the resulting patterns above the threshold (for $\sigma \ll 1$) have small amplitude and a wavelength close to $2\pi/k_c$.

If $\mathrm{Im}(\lambda) = 0$ the unstable modes are growing in time for positive values of σ but each mode is stationary in space. Thus, close to threshold, the dynamics of (5.1) can be written as

$$u = u_0 + A(x,t)\,e^{ik_c x} + A^*(x,t)\,e^{-ik_c x} + h.o.t.\,,$$

where $A(x,t)$ denotes the complex amplitude. Then, to lowest order in σ, and after rescaling, the amplitude A obeys *the real Ginzburg-Landau equation (RGLE)*:

$$\frac{\partial A}{\partial t} = \frac{\partial^2 A}{\partial x^2} + \sigma A - |A|^2 A. \tag{5.2}$$

With an additional rescaling

$$x \mapsto \sigma^{-1/2} x, \quad t \mapsto \sigma^{-1} x, \quad A \mapsto \sigma^{1/2} A,$$

the control parameter σ can be scaled out from Eq. (5.2), i.e.,

$$\boxed{\frac{\partial A}{\partial t} = \frac{\partial^2 A}{\partial x^2} + A - |A|^2 A.} \tag{5.3}$$

Notice that Eq. (5.3) arises naturally near any stationary supercritical bifurcation if the system (5.1) features translational invariance and is reflection symmetric ($x \mapsto -x$). Translational invariance, e.g., implies that (5.3) has to be invariant under $A \mapsto Ae^{i\phi}$. Notice also that Eq. (5.3) can be rewritten in the form

$$\frac{\partial A}{\partial t} = -\frac{\delta V}{\delta A^*}, \quad V = \int dx \left(\left| \frac{\partial A}{\partial x} \right|^2 - |A|^2 + \frac{1}{2}|A|^4 \right),$$

and thus, V plays role of a Lyapunov functional ($dV/dt < 0$). The next point to emphasize is that Eq. (5.3) possesses a stationary *phase winding* solution

$$A = a_0\, e^{iqx}, \qquad q^2 = 1 - a_0^2,$$

describing steady state periodic patterns with wave number slightly smaller ($q < 0$) or sligtly bigger ($q > 0$) than the critical wave number k_c.

5.2 The Complex Ginzburg-Landau Equation

Now let us consider the case $\mathrm{Im}(\lambda) := \omega_c \neq 0$, so each mode corresponds to a travelling wave. In this case we can write the solution of (5.1) as

$$u = u_0 + A(x,t)\,e^{ik_c x + i\omega_c t} + A^*(x,t)\,e^{-ik_c x - i\omega_c t} + h.o.t.\,,$$

and, after rescaling, the equation for the complex amplitude A reads

$$\boxed{\frac{\partial A}{\partial t} = (1+i\alpha)\frac{\partial^2 A}{\partial x^2} + A - (1+i\beta)|A|^2 A}, \tag{5.4}$$

where α and β are parameters. This equation is referred to as *the complex Ginzburg-Landau Equation (CGLE)*. Notice that the RGLE (5.3) is simply a special case of the CGLE (5.4) with $\alpha = \beta = 0$. Notice also, that in the limit case $\alpha, \beta \to \infty$ Eq. (5.4) reduces to the Nonlinear Schrödinger Equation, which possess, for instance, well-known soliton solutions [1].

5.2.1 Plane waves and their stability

The simplest solutions of CGLE are plane wave solutions, which take the form

$$A = a_0 \, e^{iqx + i\omega t} \,, \tag{5.5}$$

where

$$a_0^2 = 1 - q^2, \qquad \omega = -\alpha q^2 - \beta a_0^2 .$$

The expression for ω illustrates that the coefficient α and β mesure linear (the dependence of the wave's frequency on the wavenumber) and nonlinear dispersion, respectively. In order to investigate the stability of (5.5) we seek the solution in the form

$$A = \left(a_0 + \widetilde{a}_+ e^{ikx + \lambda t} + \widetilde{a}_- e^{-ikx + \lambda^* t} \right) e^{iqx + i\omega t} \,,$$

where $\widetilde{a}_\pm$ denote the amplitudes of the small peturbations. After substitution of this expression into (5.4) one can find an equation for the growth rate λ. By expanding this equation for small k (the long-wavelength limit) one obtains [1]

$$\lambda = -2iq(\alpha - \beta)k - \left[1 + \alpha\beta - \frac{2q^2(1+\beta^2)}{a_0^2} \right] k^2 + \mathscr{O}(k^3) \,. \tag{5.6}$$

Thus, travelling waves solutions are long-wave stable as long as the condition

$$1 + \alpha\beta - \frac{2q^2(1+\beta^2)}{a_0^2} > 0$$

holds. That is to say that one has a stable range of wave vectors with

$$q^2 < \frac{1 + \alpha\beta}{2\beta^2 + \alpha\beta + 3} \,,$$

including the band centre ($q = 0$) state as long as the so-called *Benjamin-Feir-Newell criterion*

$$1 + \alpha\beta > 0 \tag{5.7}$$

holds. Notice that the Benjamin-Feir instability criterion is a generalisation of *the Eckhaus instability* see Sec. 4.6.2.2 of the Chapter 4. For example, for $\alpha = \beta$, the stability condition reduces to the well-known Eckhaus condition $q^2 < 1/3$. The next

point to emphasize is that for $\alpha \neq \beta$ and $q \neq 0$ the destabilizing modes have a group velocity $v_g = 2q(\alpha - \beta)$, i.e., the instability is of a convective nature.

5.2.1.1 Plane waves: Numerical Treatment

Our goal is to solve Eq. (5.4) by means of pseudospectral method and ETD2 exponential time-stepping (D.6) (see Appendix D.1). According to the notations, introduced in Appendix D.1, Eq. (5.4) in the Fourier space becomes

$$\frac{d\widehat{A}}{dt} = \underbrace{(1 - k^2(1 + i\alpha))}_{q}\widehat{A} - \underbrace{\mathscr{F}[(1 + i\beta)|A|^2 A]}_{\mathscr{N}}, \tag{5.8}$$

i.e., scheme (D.6) can be applied:

$$\widehat{A}_{n+1} = \widehat{A}_n e^{qh} + \mathscr{N}_n \frac{(1 + hq)e^{qh} - 1 - 2hq}{hq^2} + \mathscr{N}_{n-1} \frac{-e^{qh} + 1 + hq}{hq^2}. \tag{5.9}$$

We start from the simulation of the plane waves. Let us choose parameters α and β such that there exists a stable range of wavenumbers and then simulate the CGLE with an initial condition of small noise of order 0.01 about $A = 0$. Other parameters are

`Constants`	$(\alpha, \beta) = (1, 2)$
`Domain size`	L=100
`Timestep`	$h = 0.05$
`Number of grid points`	$N = 512$

Selection of a plane wave can be seen on Fig. 5.1. One can see that $|A|$ quickly

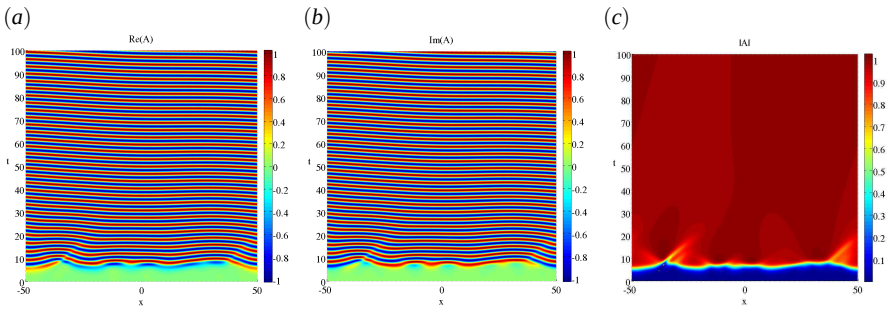

Fig. 5.1 Space-time plots of (a) Re(A), (b) Im(A) and (c) $|A|$ for the case $(\alpha, \beta) = (1, 2)$.

converges to a non-zero constant value.
In order to simulate the Benjamin-Feir instability let us consider the same parameter space but using a linearly unstable plane wave as an initial condition:

`Constants`	$(\alpha,\beta)=(1,2)$
`Domain size`	L=100
`Timestep`	$h=0.05$
`Number of grid points`	$N=512$
`Initial condition`	$A(x,0)=\sqrt{1-\left(\frac{20\pi}{L}\right)^2}\exp(i\frac{20\pi}{L}x)+\text{noise}$

The result is presented on Fig. 5.2 In can be seen that a new plane wave is selected

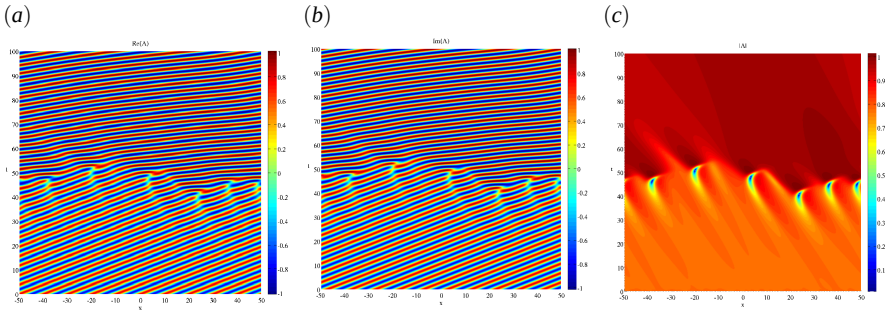

Fig. 5.2 Space-time plots of (a) Re(A), (b) Im(A) and (c) $|A|$ in the case of the Benjamin-Feir instability.

with wavenumber lying inside the band of stability. The process of selecting the new plane wave gives rise to *'defects' or phase singularities* (points where $A=0$).

5.2.2 Spatiotemporal chaos

Now let us discuss behaviour of the solutions of the one-dimensional CGLE (5.4) when the Benjamin-Feir-Newell criterion (5.7) is violated. In this region of the parameter space (α,β) several different forms of spatio-temporal chaotic or disordered states have been found [2, 19]. In particular beyond the BF instability line Eq. (5.4) exhibits so-called *phase turbulence* regime (see Fig. 5.3), which can be described by a phase equation of the Kuramoto-Sivashinsky type [1, 19]. As can be seen on Fig. 5.3 (b), in this spato-temporally chaotic state $|A|$ never reaches zero and remains saturated, so the global phase difference becomes the constant of the motion and is conserved. Moreover, Eq. (5.4) exhibits spatio-temporally disordered regime called *amplitude* or *defect turbulence*. The behaviour in this region is characterised by defects, where $|A|=0$ (see Fig. 5.4) Apart from spatio-temporal chaotic behaviour discribed above a so-called *bichaos* region can be found [19]. In this region, depending on the initial conditions, either defect-mediated turbulence or phase turbulence can be indicated.

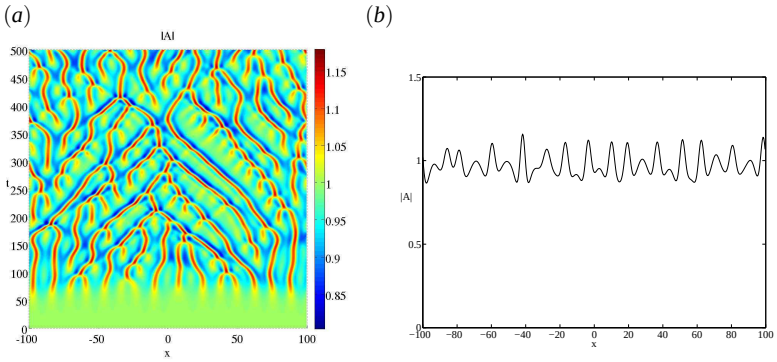

Fig. 5.3 Phase turbulence regime observed for $(\alpha, \beta) = (2, -1)$. (a) Space-time plot $|A|$. (b) The final configuration of $|A|$. Other parameters: see the Table below.

`Constants`	$(\alpha, \beta) = (2, -1)$
`Domain size`	L=200
`Timestep`	$h = 0.05$
`Number of grid points`	$N = 512$
`Initial condition`	$A(x,0) = 1.0 + \text{noise}$

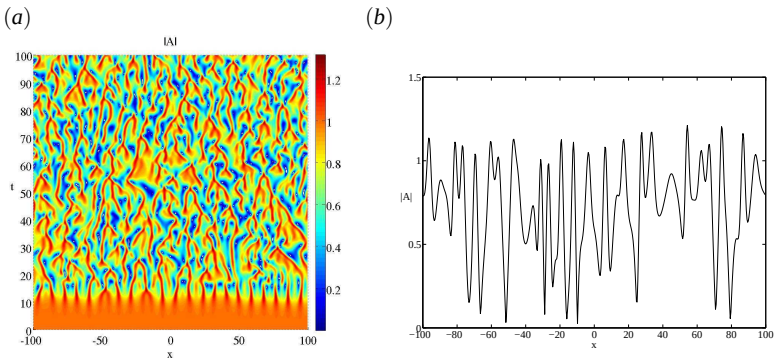

Fig. 5.4 Defect turbulence regime observed for $(\alpha, \beta) = (2, -2)$. (a) Space-time plot $|A|$. (b) The final configuration of $|A|$. Other parameters: see the Table below.

`Constants`	$(\alpha, \beta) = (2, -2)$
`Domain size`	$L = 200$
`Timestep`	$h = 0.05$
`Number of grid points`	$N = 512$
`Initial condition`	$A(x,0) = 1.0 + \text{noise}$

5.2.3 The intermittency regime

The linear stability of the plane wave solution (5.7) does not exclude the existence or coexistence of the other non-trivial solutions of (5.4). For example, the regime of spatio-temporal intermittency, where defect chaos coexists with stable plane wave was discussed in details in [19]. There, in order to avoid the stable plane wave solution, initial condition was composed of one or several localised pulses of amplitude. After a rather short transient, the typical solution consist of localized structures, separating lager regions of almost constant amplitude which are patches of stable plane wave solutions (see Fig. 5.5). Figure 5.6 shows a more complicated intermittency

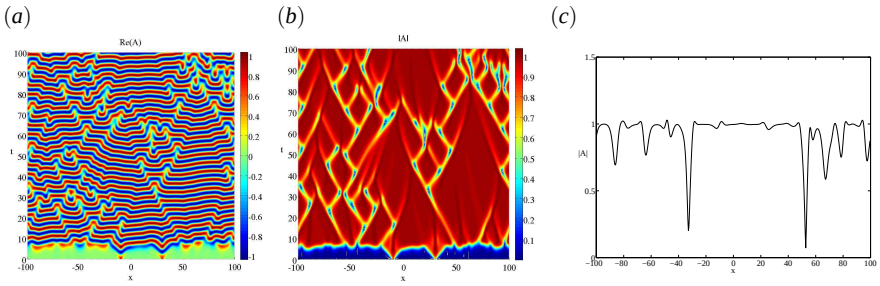

Fig. 5.5 The intermittency regime observed for $(\alpha, \beta) = (0.5, -1.5)$. (a) Space-time plot Re$(A)$; (b) Space-time plot $|A|$; (c) The final configuration of $|A|$. Other parameters: see the Table below.

`Constants`	$(\alpha, \beta) = (0.5, -1.5)$
`Domain size`	$L = 200$
`Timestep`	$h = 0.05$
`Number of grid points`	$N = 512$
`Initial condition`	$A(x,0) = \mathrm{sech}((x+10)^2) + 0.8 * \mathrm{sech}((x-30)^2) + \mathrm{noise}$

scenario observed for $(\alpha, \beta) = (0, -4)$. In this case the spatial extension of the system is broken by irregular arrangements of stationary hole- and shock-like objectes separated by turbulent dynamics.

5.2.4 Coherent structures

Apart from plane waves, Eq. (5.4) provides a lager variety of so-called *coherent structures*. These solutions are either localized or consist of domains of regular patterns connected by localized defects or interfaces. One-dimensional coherent structure can be written in the form [56]

$$A(x,t) = a(x - vt)\exp(i\phi(x - vt) - i\omega t)\,. \tag{5.10}$$

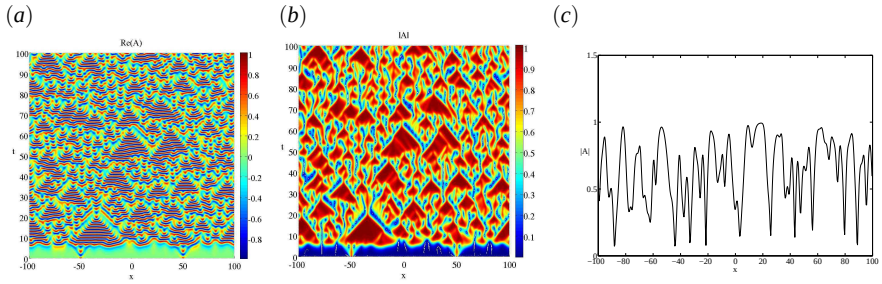

Fig. 5.6 The intermittency regime observed for $(\alpha,\beta)=(0,-4)$. (a) Space-time plot Re(A); (b) Space-time plot $|A|$; (c) The final configuration of $|A|$. Other parameters: see the Table below.

`Constants`	$(\alpha,\beta)=(0,-4)$
`Domain size`	$L=200$
`Timestep`	$h=0.05$
`Number of grid points`	$N=512$
`Initial condition`	$A(x,0)=\mathrm{sech}((x+L/4)^2)+0.8*\mathrm{sech}((x-L/4)^2)+\mathrm{noise}$

After substitution of this equation into (5.4) lead to the system of three ordinary differential equations with respect to variables (see [56]for more details)

$$q(\xi)=\partial_\xi\phi,\quad \kappa(\xi)=\partial_\xi a/a,\quad \partial_\xi a=\partial a/\partial_\xi\,,$$

where $\xi=x-vt$. The resulting system of ODE's can be discussed in terms of dynamical system in pseudo-time ξ with three degrees of freedom. Accordingly to the assymptotic states the localized coherent structues can be classified as *fronts, pulses, source (holes) and sinks (shoks)*. The best known example of sink solutions are *Bekki-Nozaki holes* [3], illustrated on Fig. (5.7). These structures asymptotically connect plane waves of different amplitude and wavenumber and make a one-parameter family of solutions of CGLE [37]. As can be seen on Fig. 5.7 in the case of several holes they are separated by shoks [1].

5.2.5 The CGLE in 2D

The two-dimensional version of the CGLE reads

$$\frac{\partial A}{\partial t}=(1+i\alpha)\triangle A+A-(1+i\beta)|A|^2A, \tag{5.11}$$

where A is a complex field. Apart of two-dimensional analogues of defect and phase turbulence Eq. (5.11) has a variety of coherent structures [1, 20]. Among others Eq. (5.11) possesses two-dimensional cellular structures known as *frosen states* (see Fig. (5.8)). They appear in the form of quasi-frosen arrangments of spiral defects

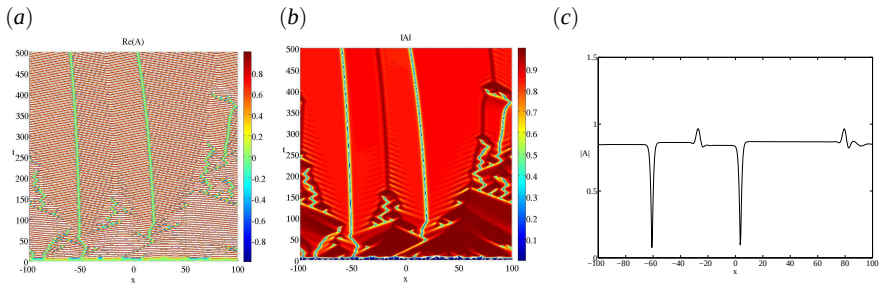

Fig. 5.7 The moving hole-shock pair observed for $(\alpha, \beta) = (0, 1.5)$. (a) Space-time plot Re$(A)$; (b) Space-time plot $|A|$; (c) The final configuration of $|A|$. Other parameters: see the Table below.

`Constants`	$(\alpha, \beta) = (0, 1.5)$
`Domain size`	$L = 200$
`Timestep`	$h = 0.05$
`Number of grid points`	$N = 512$
`Initial condition`	$A(x,0) =$ noise of the amplitude 0.01

surrounded by shock lines. Note that $|A|$ in this regime is stationary in time. For a

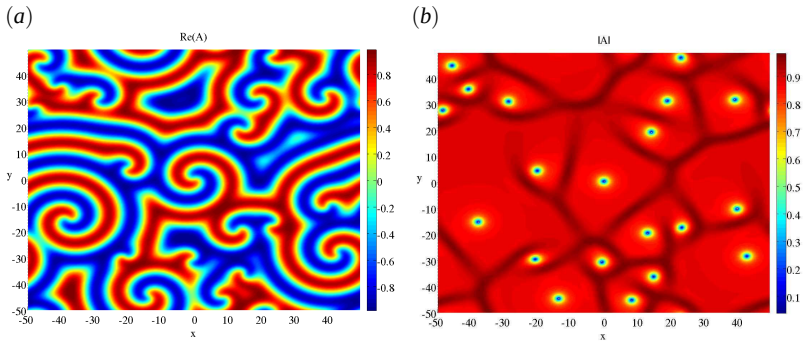

Fig. 5.8 Two-dimensional cellular structures observed for $(\alpha, \beta) = (0, 1.5)$. (a) Space-time plot Re$(A)$; (b) Space-time plot $|A|$. Other parameters: see the Table below.

`Constants`	$(\alpha, \beta) = (0, 1.5)$
`Domain size`	$L = [-100, 100] \times [-100, 100]$
`Timestep`	$h = 0.05$
`Number of grid points`	$N = 256$
`Initial condition`	$A(x,0) =$ noise of the amplitude 0.01

complete review of the phase diagram for the two-dimensional CGLE see [20].